

Response Reduction of Base-Isolation System Against Near-Fault Pulse and Long-Period Ground Motions



H. Fujitani & Y. Mukai

Kobe University, Kobe, Japan

T. Tomizawa

Kozo Keikaku Engineering Inc., Tokyo, Japan

K. Hirata & Y. Mazuka

Kobe University, Kobe, Japan

H. Fujii

Daiwa House Industry Co., LTD (former graduate student of Kobe University), Osaka, Japan

SUMMARY:

Base-isolation systems show high performance of the reduced floor acceleration and deformation of superstructures during periods of large earthquake ground motion. However, against near-fault pulse ground motions of intra-plate earthquakes or long-period ground motions of inter-plate earthquakes, results of recent studies show that excessively great displacement occurs in the base-isolation layer. Base-isolation systems present a risk of collision with the retaining wall and an increase of the story shear force and floor acceleration of the superstructure. Furthermore, the shear strain of laminated rubber bearings must be controlled to be smaller than the critical value.

Some methods that have been proposed and verified as described herein reduce the response displacement to avoid collision with the retaining wall, thereby maintaining the safety and function of base-isolation systems without the increased floor acceleration of superstructures against such specific ground motions. The proposed methods were validated using numerical simulations and shaking table tests.

Keywords: Base-isolation, Near-fault pulse, Long-period ground motion, Semi-active control, Passive control

1. INTRODUCTION

1.1. Background

Near-fault pulse ground motions of intra-plate earthquakes, which have a predominant period of 1–2 s, were observed during the 1994 Northridge Earthquake and the 1995 Hyogo-ken Nambu Earthquake. This near-fault pulse ground motion caused large deformation in the base-isolation layer of the base-isolation system (Heaton et al. (1995)). In the Osaka city area, offices of Osaka Prefecture and Osaka City predicted ground motions and publicized the earthquake damage assessment based on their own research activities to provide information against a possible “Uemachi-fault” earthquake as a near-field earthquake (Osaka Prefectural Government (2007), Taga, K. et al. (2011) (2012)). However, long-period ground motions of inter-plate earthquakes have been observed in recent years. Such long-period ground motions engender the resonance response of the base-isolation system. Consequently, excessively large displacement occurs in the base-isolation layer.

Base-isolation systems present a risk of collision with retaining walls and an increase of the story shear force and floor acceleration of the superstructure. Furthermore, the shear strain of laminated rubber bearings must be controlled as smaller than the critical value, for example 400%. Base-isolation systems with rubber bearings confronting more than 400% shear strain are quite unstable and dangerous.

1.2. Objectives

As described in this paper, some methods that have been proposed and verified as described herein reduce the response displacement to avoid collision with the retaining wall, thereby maintaining the safety and function of base-isolation systems without the increased floor acceleration of superstructures against such specific ground motions. The proposed methods were validated using numerical simulations and shaking table tests.

First, the effect of passive control by additional hydraulic damper which works against larger deformation of base-isolation layer with dynamic mass damper (DMD) is examined in Chapter 3. Then, the effect of passive and semi-active control by rotational inertia mass damper (VRIMD) filled with MR fluid is examined in Chapter 4. Finally, the effect of semi-active control by MR damper especially against long-period ground-motion is examined in Chapter 5.

2. EARTHQUAKE GROUND MOTIONS AND MODEL STRUCTURE

2.1. Earthquake ground motions

In this study, earthquake ground motions of six kinds are adopted to examine the effects of control methods. First is a group of the ground motions that are popular for evaluation of high-rise or base-isolated building presumed as a very rare case with a return period of 500 years in Japan. Those are adjusted that the peak ground velocity is 0.50 m/s (Nos. 1 and 2 shown in Table 1). Second is a group of ground motions observed in Kobe City when the Hyogoken Nambu Earthquake occurred. Those have characteristic of near-fault pulse earthquake ground motions (Nos. 3 and 4 in Table 1). Third is the artificial ground motion presuming a Future Uemachi Earthquake (No. 5 in Table 1) (Taga et al. (2011) (2012)). This has characteristics of near-fault pulse earthquake ground motions. Fourth is the artificial ground motion presuming a Future Nankai Earthquake (No. 6 in Table 1) (Kawabe & Kamae (2004)). This has characteristics of long-period ground motion. Earthquake response spectra are presented in Fig. 1.

Table 1. List of earthquake ground motions

| Earthquake ground motion | Character | Peak ground acceleration (m/s^2) | Peak ground velocity (m/s) |
|--|------------------|--------------------------------------|----------------------------|
| No.1) El Centro 1940 NS (Peak ground velocity = 0.5 m/s) | | 6.01 | 0.50 |
| No.2) Hachinohe 1968 NS (Peak ground velocity = 0.5 m/s) | | 3.54 | 0.50 |
| No.3) JMA Kobe 1995 NS | Near fault pulse | 8.18 | 0.92 |
| No.4) Takatori 1995 NS | Near fault pulse | 6.06 | 1.23 |
| No.5) UMT A4 EW3 (Future Uemachi Earthquake) | Near fault pulse | 3.63 | 0.72 |
| No.6) Rokko Island (Future Nankai Earthquake) | Long period | 1.21 | 0.13 |

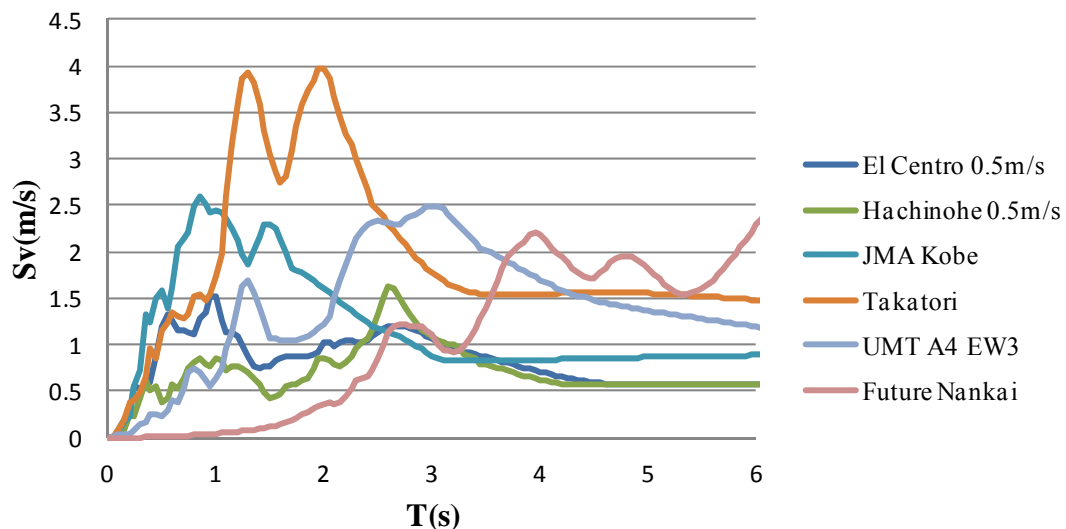


Figure 1. Earthquake response Spectra ($h=0.05$)

2.2. Model Building

A four-storey reinforced concrete base-isolated residential building is modelled to a single-degree-of-freedom system. The building characteristics are shown in Table 2. The building is supported by natural rubber bearings. One hydraulic damper is installed for each direction. The hydraulic damper characteristic is presented in Fig. 2.

Table 2. Specifications of building

| | |
|-----------------------------------|-----------------------|
| Mass | 2.0×10^6 kg |
| Stiffness of base-isolation layer | 5.0×10^6 N/m |
| Natural period of base-isolation | 4.0 sec |
| Damping ratio | 0.03 |

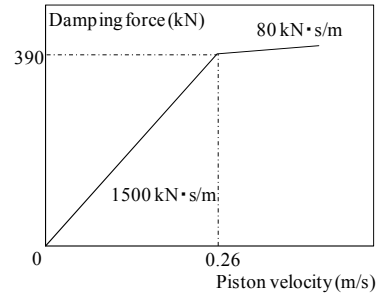


Figure 2. Velocity-force relationship of hydraulic damper

3. PASSIVE CONTROL BY ADDITIONAL HYDRAULIC DAMPER WITH DYNAMIC MASS

3.1. Concept

The model building has one hydraulic damper (Fig. 3). However, more dampers are necessary to reduce response displacements when near-fault pulse ground motions strike the building. If some hydraulic dampers are installed to the base-isolation layer, then the floor acceleration of the superstructure is increased as presented in Fig. 3, even if the response displacement of base-isolation layer is reduced. Therefore, increased acceleration sacrifices an important advantage of the base-isolation system by which vibration of the superstructure is calm in the event of ordinary earthquake ground motion, for example, for earthquake ground motions No.1 and No. 2 shown in Table 1.

The authors propose a method by which additional hydraulic dampers are installed to the base-isolation layer and are activated only when the response displacement is greater than the boundary displacement. Furthermore, the dynamic mass damper (DMD) is installed to reduce the floor acceleration.

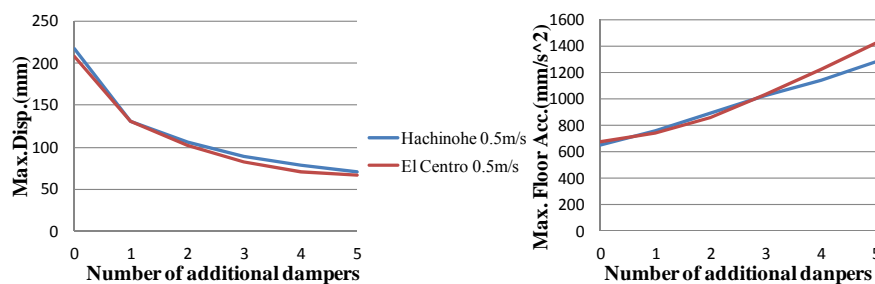


Figure 3. Maximum response displacements and floor accelerations on number of additional dampers

3.2. Dynamic Mass Damper (DMD)

A structural control system using a dynamic mass damper (DMD) is proposed, with effects verified by Furuhashi and Ishimaru (Furuhashi et al. (2010)). The authors expect that DMDs reduce or prevent increases of floor acceleration of the base-isolation system when many dampers are installed in the

base-isolation layer to reduce response displacements because DMD produces negative stiffness. Fig. 4 presents the dynamic mass concept. The mass of the larger wheel m_d is presumably distributed only at the edge of the larger wheel (B). The amplification ratio of β is the ratio of the radius of the larger wheel (B) to the smaller wheel (A). The mass m_d of the larger wheel (B) is amplified to the magnitude of $\beta^2 m_d$ at the position of the smaller wheel (A). $\beta^2 m_d$ is named the “Dynamic Mass” and the magnitude of dynamic mass is expressed as m' ($=\beta^2 m_d$) by Furuhashi et al.

3.3. Analytical Study

An analytical study was conducted using earthquake ground motions of three kinds: No. 4 (observed,

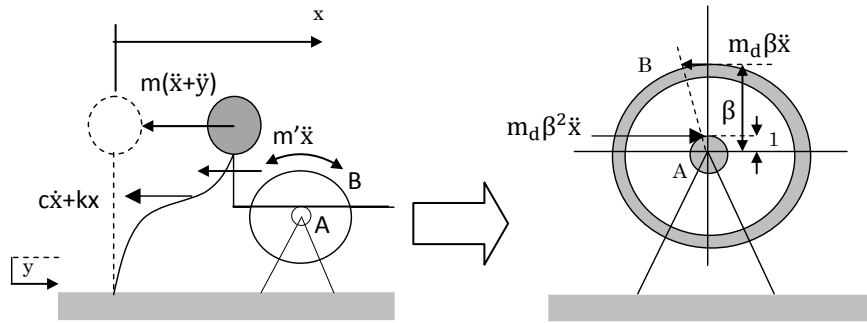


Figure. 4 Concept of dynamic mass damper

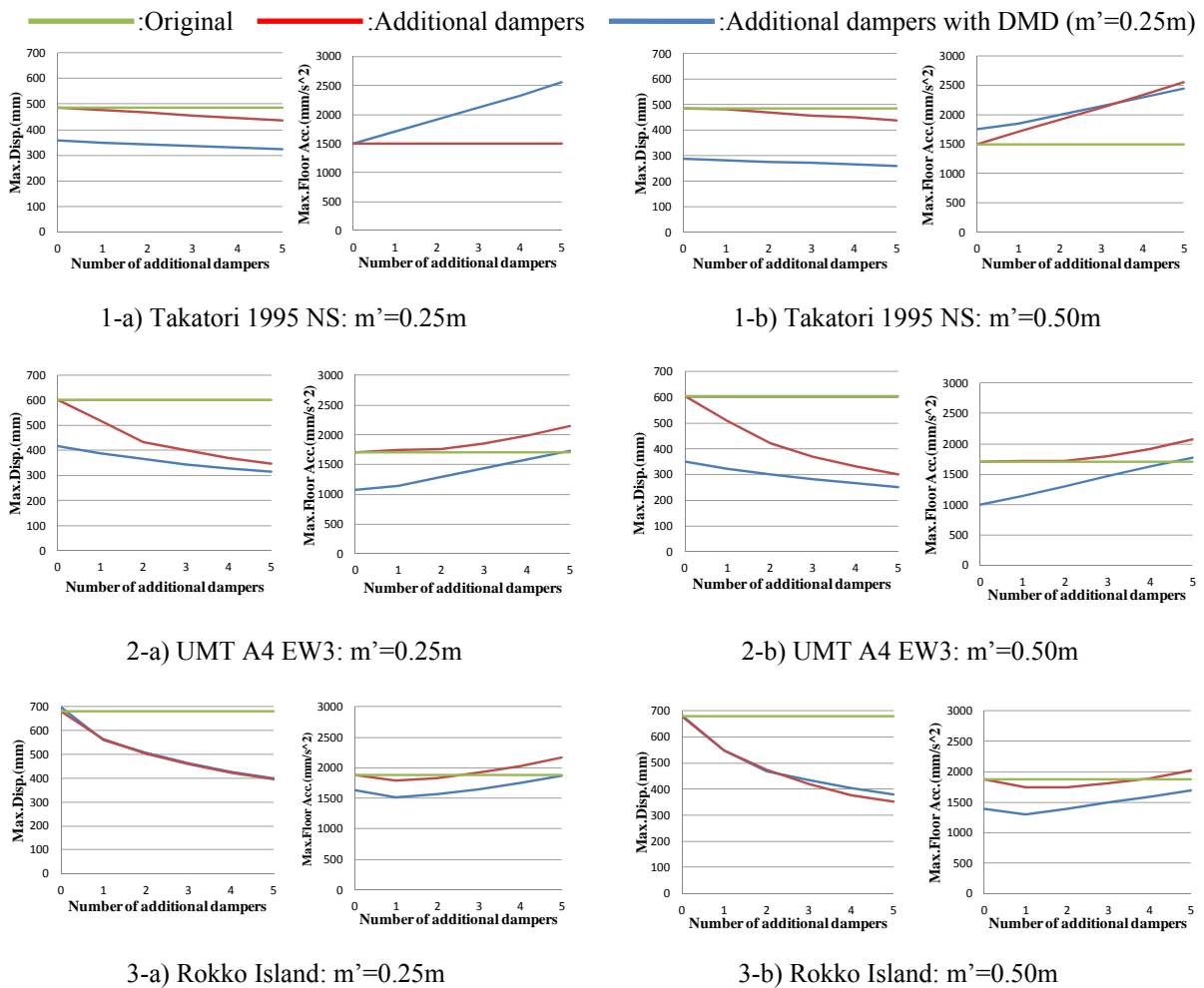


Figure 5. Maximum response displacements and maximum floor accelerations against near-fault pulse and long-period ground motions in case of $m'=0.25 m$ and $0.50 m$ of DMD

near-fault pulse), No. 5 (artificial, near-fault pulse) and No. 6 (artificial, long-period) in Table 1 to examine the response reduction effect of the proposed method as follows.

- Hydraulic dampers (Table 2) added to the base-isolation layer one by one.
- DMDs of $m^*=0.25 m$ and $0.50 m$ (m , real mass of the structure) are installed.

The results are portrayed in Fig. 5.

3.4. Discussion

For almost all cases in which only a hydraulic damper is added one by one (—), response displacements are reduced and floor accelerations are increased proportionally to the increase of the number of dampers (Fig. 5). Then, for installing DMD (—) added to the base-isolation layer, both response displacements are reduced sufficiently and floor acceleration is reduced to be less than those of the original buildings (—), except 1-a) and 1-b).

The combination of DMD and additional hydraulic dampers is effective for reducing response displacements without increasing floor acceleration against near-fault pulse ground motions and long-period ground motions. Installing too many DMDs ($m^*=0.5 m$) is ineffective against extremely large near-fault pulse ground motion like Takatori (1-b).

4. PASSIVE AND SEMI-ACTIVE CONTROL BY ROTATIONAL INERTIA MASS DAMPER

4.1. Concept

In Chapter 3, the floor acceleration was increased when hydraulic dampers were added one by one. Therefore, the authors discuss the effect of rotational inertia and the effect of viscosity. For this purpose, a variable rotational inertia mass damper (VRIMD) was manufactured for trials. The VRIMD structure is presented in Fig. 6. The specifications are depicted in Fig.7 and Table 3. The MR fluid is installed between the flywheel and case of this damper. The viscosity of MR fluid and damper force is increased when the electric current is induced to the electromagnet (Fig. 8). Therefore, by controlling the value of the electric current, semi-active control of the variable viscosity is realized. In this chapter, analytical studies using this VRIMD are conducted.

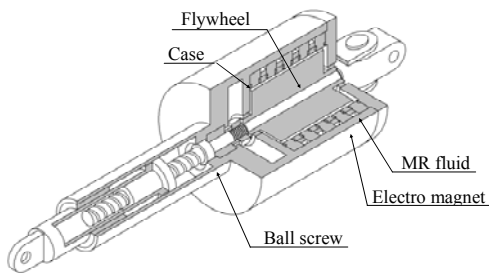


Figure 6. Structure of VRIMD

Table 3. Specifications of VRIMD

| | | |
|---------------------------|-------------------|------------------|
| Stroke | 250 (± 125) | mm |
| Max. damper force | 100 | kN |
| Max. piston acceleration | 5.0 | m/s ² |
| Max. piston velocity | 0.7 | m/s |
| Inertia mass | 30 | ton |
| | 2.4 | |
| Damping coefficient (0 A) | 76.5 | kN·s/m |

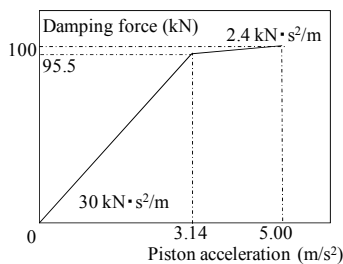


Figure 7. Acceleration-force relationship of VRIMD (without MR fluid)

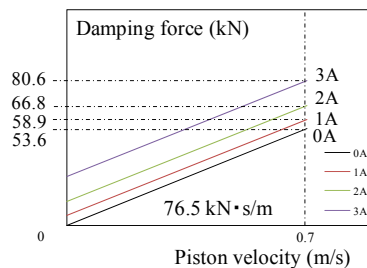


Figure 8. Velocity-force relationship of VRIMD

4.2. Analytical study

Analytical study was conducted against earthquake ground motions of five kinds: No. 1, No. 2, No. 3 (observed, near fault pulse), No. 4 (observed, near fault pulse), and No. 5 (artificial, long-period). Fig. 9 portrays the results. Series from 1-a) to 1-c) show the effects of the rotational inertia only. Series 2-a) to 2-c) show the effect of the rotational inertia with high viscosity by application of 3A electric current to the electric current. Series of 3-a) to 3-c) show the effects of variable control using the optimal regulatory control (Yang, J. N. (1975)) to control the viscosity. Eqn. (4.1) is the evaluation function.

$$J = \frac{1}{2} \int_0^{\infty} [\alpha_d x^2 + \alpha_v \dot{x}^2 + \alpha_a (\ddot{x} + \ddot{z})^2 + \gamma u^2] dt \quad (4.1)$$

α_d , α_v , α_a , and γ respectively represent the weighting coefficients related to displacement, velocity, acceleration, and control force. Herein, α_d , α_v , α_a , and γ are respectively set equal to 1.0. Furthermore, the electric current was controlled to be On-Off by the rule of Skyhook Control (Karnopp et al. (1941)).

4.3. Discussion

Response displacements are reduced and floor accelerations are increased by the increase of quantities of rotational inertia against both near-fault pulse and long-period ground motions (1-a, 1-b, 1-c). Then, when high-viscosity is given by application of electric current to the electromagnet VRIMD, response displacements are reduced in cases of UMT A4 EW3 and Future Nankai, but floor acceleration is increased in those cases, compared to (1-a, b, c) and (2-a, b, c).

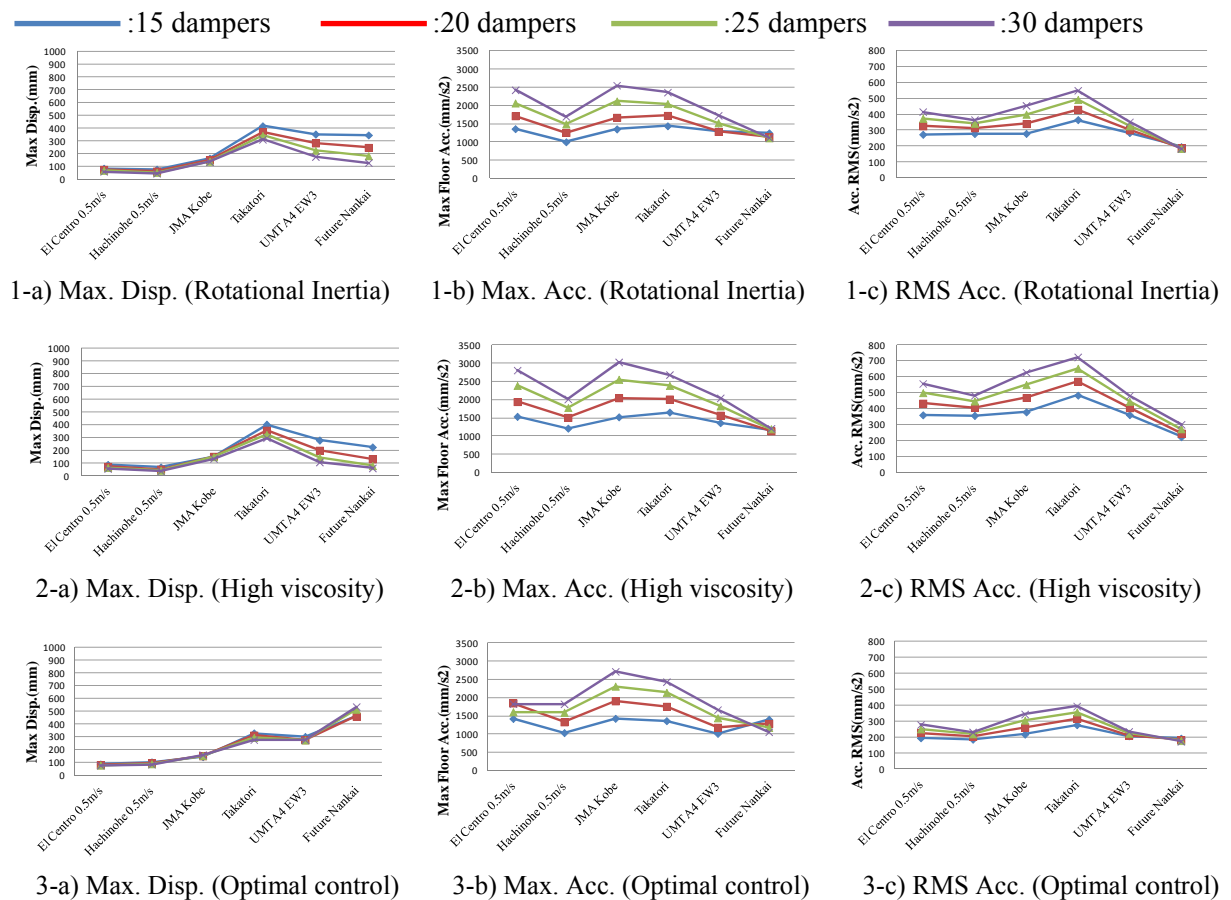


Figure 9. Response values controlled by VRIMD

When semi-active optimal control was conducted, floor acceleration was reduced in many cases, but with respect to a Future Nankai earthquake, response displacements were not reduced even by the semi-active control, comparing (2-a, b, c) and (3-a, b, c).

5. SEMI-ACTIVE CONTROL AGAINST LONG-PERIOD GROUND MOTION

Against long-period ground motions of inter-plate earthquakes, semi-active control is effective to reduce the response displacement without the increased floor acceleration of superstructures. The efficacy was verified by shaking table tests by using Magneto-rheological (MR) damper (Rabinow, J. (1948)). Authors used the long-period ground motion caused by the Future Nankai Earthquake (Fujitani, H., Kawabe, H., et al. (2007)). It was synthesized supposing the site of central part of Kobe City.

5.1. Shaking Test Setting

Shaking table tests were conducted at the Building Research Institute. Photo 1 and Table 4 show test specimens of a base isolation system with two degrees of freedom in the superstructure system. The superstructure is supported by four roller bearings. The restoring force is given by two laminated rubber bearings. The second floor is supported by four laminated rubber bearings, and the restoring force is given by them. The MR damper is installed between the first floor and the base frame.

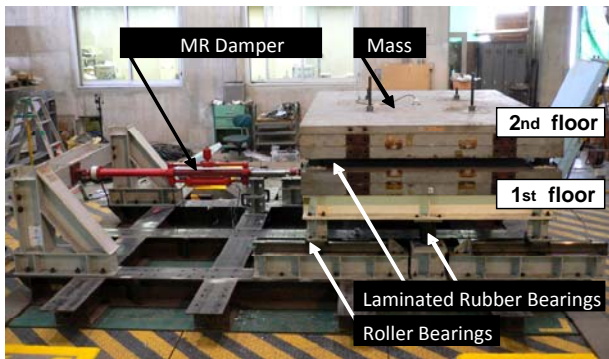


Photo 1. Test system of base isolation (2 DOF)

Table 4. Dimensions of testing system (2DOF)

| 2nd layer | |
|---------------------------------------|------------|
| Mass | 8100 kg |
| Stiffness of laminated rubber bearing | 350 kN/m |
| Damping coefficient | 3.0 kN·s/m |
| Natural period (only super structure) | 0.95 s |
| Base-isolated layer | |
| Mass | 6300 kg |
| Stiffness of laminated rubber bearing | 50 kN/m |
| Damping coefficient | 3.0 kN·s/m |
| Friction force of roller bearing | 0.3 kN |
| Natural period | 3.4 s |

5.2. MR damper

The maximum damping force of the MR damper used for this study is 10 kN. Its stroke is +/-300 mm as depicted in Fig. 10 and Table 5. Figure 11 presents the force–displacement relation of the MR damper. The damping force is generated along the volume of electric current mainly and the loop shape shows that the damping force is not so much smaller in case the maximum displacement (Piston velocity is zero) than the maximum force shown in Fig. 11. The MR damper is expressed simply using the Bingham plastic model, as presented in Fig. 13, and the relation between the damper force “ F_{MR} ” and the electric current is approximated as Eqn. (5.1). In Eqn. (5.1), “ I ” is electric current (a), and “ v ” is the piston velocity (m/s). Figure 12 presents the simulated force–displacement relationship. The Bingham plastic model and Eqn. (5.1) shows good mutual agreement..

5.3. Control Method

The authors adopted the Optimal Regulatory Control (Yang, J. N. (1975)) to control the MR damper. Eqn. (5.2) is the evaluation function.

$$J = \frac{1}{2} \int_0^{\infty} [\alpha_d x^2 + \alpha_v \dot{x}^2 + \alpha_a (\ddot{x} + \ddot{z})^2 + \gamma u^2] dt \quad (2.2)$$

α_d , α_v , α_a , and γ are weighting coefficients, respectively related to displacement, velocity, acceleration, control force. Herein, α_d , α_v , α_a , and γ were set in control of two types, as shown in Table 4.

Results of shaking table tests show that control Type 1 was effective to reduce the floor acceleration, and control Type 2 was effective to reduce the relative displacement of the base-isolation layer. Therefore, the authors propose switching control between Type 1 and Type 2, as depicted in Fig. 14 and Table 7.

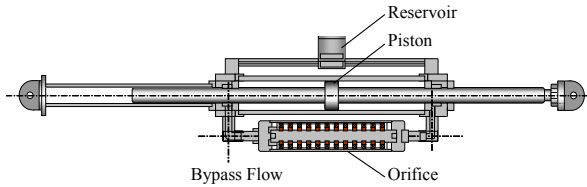


Figure 10. Structure of MR damper

Table 5. Dimensions of MR damper

| | | |
|--|-------|------|
| Maximum force | 10 | kN |
| Stroke | ±300 | mm |
| Max. electric current of electromagnet | 5.0 | A |
| Magneto-rheological fluid | Bando | #230 |

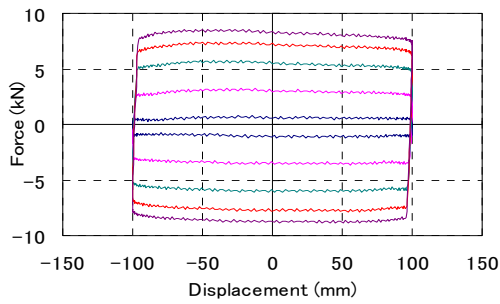


Figure 11. Test result of the MR damper

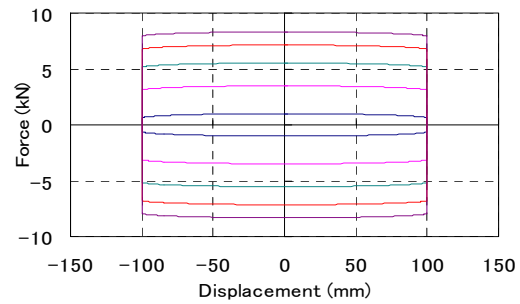


Figure 12. Simulated force-displacement relationship

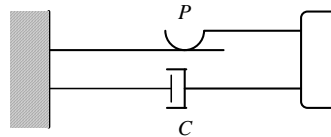


Figure 13. Bingham plastic model

$$F_{MR} = \text{sign}(v)(-0.198 \cdot I^2 + 2.684 \cdot I + 0.553) + 1.500 \cdot v \quad (2.1)$$

Table 6. Weighting Coefficients in Control Type 1 and Control Type 2

| | α_d | α_v | α_a | γ |
|--------|------------|------------|------------|----------|
| Type 1 | 1 | 1 | 1 | 0.01 |
| Type 2 | 1 | 100 | 1 | 0.01 |

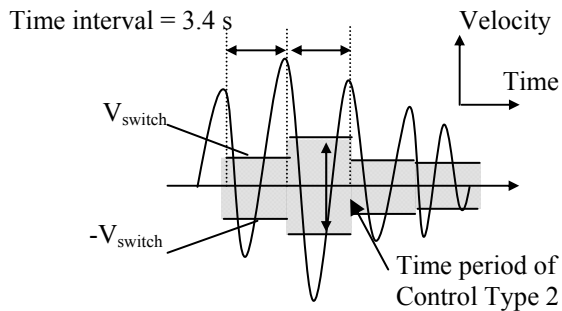


Figure 14. Outline of switching weighting coefficients

Table 7. Boundary velocity V_{switch} to change

| Maximum velocity of base-isolation layer : V_m (m/s) | V_{switch} (m/s) |
|--|---------------------------|
| ~0.1 | 0.05 |
| 0.1~0.2 | 0.10 |
| 0.2~0.3 | 0.15 |
| 0.3~0.4 | 0.20 |
| 0.4~ | 0.25 |

The procedure of switching control Type 1 and Type 2 is the following:

- 1) Sample the absolute value of relative velocity of the base-isolation layer and find the maximum value V_m in each time interval, which is equal to natural period of the structure ($= 3.4$ s)
- 2) Determine the value V_{switch} depending on V_m using Table 7

5.4. Results and Discussion

Figs. 15-18 present test results of switching control between Type 1 and Type 2 in the case of the Future Nankai Earthquake compared with other ground motions. The maximum response displacement was reduced from 94.9 mm to 25.1 mm (73% reduction) by optimal control switching Type 1 and Type 2, whereas the maximum floor acceleration is increased from 554 mm/s² to 677 mm/s² (22% increase) (Fig. 15). In contrast, for El Centro 1940 NS (Fig. 16), JMA Kobe 1995 NS (Fig. 17) and Hachinohe 1968 NS (Fig.16), both the maximum response displacement and the maximum floor response are almost identical in Type 1 and switching Types 1 and 2. Therefore, this optimal regulatory control method with switching weighting coefficients depending on response velocity works better against long-period ground motion without disturbing the other cases.

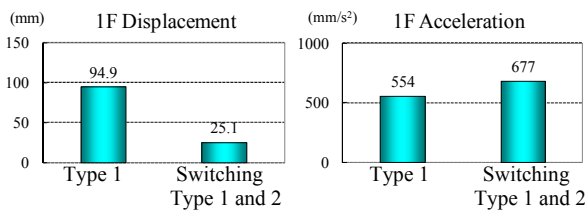


Figure 15. Results (Future Nankai NS 30%)

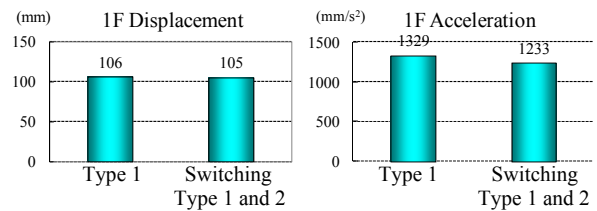


Figure 16. Results (El Centro 1940 NS 100%)

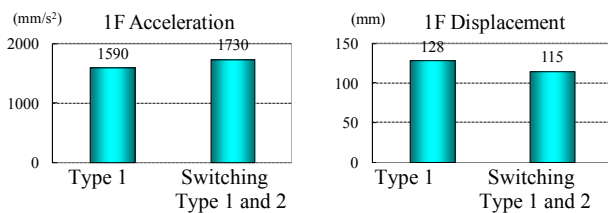


Figure 17. Results (JMA Kobe 1995 NS 0.5m/s)

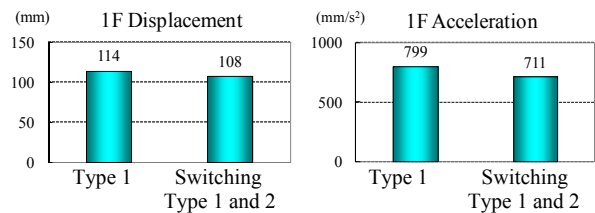


Figure 18. Results (Hachinohe 1968 NS 100%)

6. CONCLUSIONS

Some methods that have been proposed and verified as described herein reduce the response displacement, thereby maintaining the safety and function of base-isolation systems without the increased floor acceleration of superstructures against near-fault pulse and long-period ground motions.

One is the passive control by additional hydraulic damper with dynamic mass (DMD). Both response displacements are reduced sufficiently and floor acceleration is reduced to be less than those of the original buildings. The combination of DMD and additional hydraulic dampers is effective for reducing response displacements without increasing floor acceleration against near-fault pulse and long-period ground motions.

Second is the passive and semi-active control using variable rotational inertia mass damper (VRIMD). Response displacements are reduced and floor accelerations are increased by the increase of quantities of rotational inertia and viscosity against both near-fault pulse and long-period ground motions. When semi-active optimal control was conducted, floor accelerations were reduced in many cases, but with

respect to a long-period ground motion, response displacements were not reduced by the semi-active control.

Third is the semi-active control by MR damper composed of piston and cylinder. Response displacements are reduced dramatically by optimal control switching Type 1 and Type 2, whereas the maximum floor acceleration is increased a little against a long-period ground motions.

Results show that a base-isolation system excited by a near-fault pulse or long-period ground motions can be controlled using high-performance passive control and semi-active control.

AKNOWLEDGEMENT

This work was supported by the Grant in Aid for Scientific Research (C) of the Japan Society for the Promotion of Science (JSPS). The variable rotational inertia mass damper (VRIMD) was manufactured for trials by SANWA TEKKI CORPORATION. In this study, the shaking table tests were conducted at the Building Research Institute. The authors express their appreciation to Dr. Taiki Saito and Mr. Namihiko Inoue of the Building Research Institute for their kind assistance. The authors express their appreciation to Prof. Hidenori Kawabe of Kyoto University for his providing data of ground motions and Dr. Takeshi Hiwatashi for his assistance for shaking table tests.

REFERENCES

- Fujitani, H., Kawabe, H., Inoue, N. and Furuta, T. (2006). Response control of base-isolated building against strong ground motions of future Nanaki and Yamasaki fault earthquake (Part 1) Research objective and prediction of ground motions. *Summaries of Technical Papers of Annual Meeting, Architectural Institute of Japan*. **B-2**: 693-694. (in Japanese)
- Furuhashi, T., Hata, I. & Ishimaru, S. (2010). Response Control Design Method by Making Use of Dynamic Mass. *Fifth World Conference on Structural Control and Monitoring*. : 5WCSCM-278.
- Hall, J. F., Heaton, T. H., Halling, M. W. and Wald, D. J. (1995). Near-Source Ground Motion and its Effects on Flexible Buildings. *Earthquake Spectra*. **11.4**: 569-605.
- Kamae, K., Kawabe, H. & Irikura, K. (2004). Strong ground motion prediction for huge subduction earthquake using a characterized source model and several simulation techniques. *Thirteenth World Conference on Earthquake Engineering (13WCEE)*. : Paper No. 655.
- Karnopp, D., Crosby, M. J. and Harwood, R. A. (1941). Vibration Control Using Semi-Active Force Generators. *Journal of Engineering for Industry. Transactions of ASME* : 619-626.
- Osaka Prefectural Government. (2007). Osaka Prefectural Government's Comprehensive Study Report on Natural Disaster Damage and on Countermeasures. (in Japanese)
- Rabinow, J. (1948). The Magnetic Fluid Clutch. *AIEE Transaction* **67**: 1308.
- Taga, K., Kamei, I., Sumi, A., Kondo, K., Hayashi, Y., Miyamoto, Y. and Inoue, K. (2011). Research on Design Input Ground Motion and Design Method of Building for Uemachi Fault Earthquake. *Summaries of technical papers of Annual Meeting AIJ*: 127-130, (in Japanese)
- Taga, K., Tada, M., Shirasawa, Y., Ichinohe, Y. and Hashida, T. (2012). Use of Ultra-high Strength Steel in Building Frames Aiming at Major Countermeasure for Earthquakes. *Fifteenth World Conference on Earthquake Engineering (15WCEE)*. (10 pages)
- Tomizawa, T., Fujitani, H., Mukai, Y., Hirata, K., Shibata, K. & Sato, Y. (2012). Response Control by using Rotational Inertia Mass Damper filled with MR fluid. *Summaries of technical papers of Annual Meeting AIJ*. **B-2**: (4 pages) (in Japanese)
- Yang, J.N. (1975). Application of Optimal Control Theory to Civil Engineering Structures. *Journal of The Engineering Mechanics Division* **EM6**: 819-838.